Original Article

Histone demethylase KDM5A regulates the functions of human periodontal ligament stem cells during periodontitis via the miR-495-3p/HOXC8 axis

Fang Niu [a, *], Jing Xu [b], Yujuan Yan [c]

[a] Department of Oral Implantology and Prosthodontics, The First Affiliated Hospital of Zhengzhou University, Zhengzhou, Henan Province, 450000, PR China
[b] Department of Oral Orthodontics, The First Affiliated Hospital of Zhengzhou University, Zhengzhou, Henan Province, 450000, PR China
[c] Department of Oral Prosthodontics, The First Affiliated Hospital of Zhengzhou University, Zhengzhou, Henan Province, 450000, PR China

A R T I C L E   I N F O

A B S T R A C T

Introduction: Periodontitis is the sixth most common human disease and epigenetic regulation is identified to affect the functions of stem cells. This research aims to analyze the role of histone demethylase Lysine-specific demethylase 5A (KDM5A) in human periodontal ligament stem cells (hPDLSCs) with periodontitis.
Methods: hPDLSCs were treated with porphyromonas gingivalis-lipopolysaccharide (Pg-LPS) and subjected to osteogenic induction. The expression of KDM5A was detected by RT-qPCR and Western blot. Then, KDM5A expression patterns in hPDLSCs were measured and then silenced using shRNA to explore its role in osteogenic differentiation (OD), proliferation, and migration of hPDLSCs. ChIP assay was used to analyze the relationship between KDM5A and miR-495-3p, Western blot was used to detect H3K4me3 and RT-qPCR was used to detect miR-495-3p expression. CPI-455 (specific KDM5 inhibitor) was adopted to confirm the role of H3K4me3, and dual-Luciferase assay indicted the relationship between miR-495-3p and homeobox C8 (HOXC8). A functional rescue experiment was designed to analyze the role of miR-495-3p in hPDLSCs with periodontitis.
Results: KDM5A was highly expressed in LPS-treated hPDLSCs. Downregulation of KDM5A promoted OD, proliferation, and migration of hPDLSCs. Mechanically, KDM5A inhibited miR-495-3p expression by demethylation of H3K4me3 to enhance HOXC8 transcription. Downregulation of miR-495-3p could weaken the effect of sh-KDM5A to promote OD, proliferation, and migration of hPDLSCs.
Conclusions: KDM5A could bind to the miR-495-3p promoter and inhibit miR-495-3p expression by demethylation of H3K4me3 to enhance HOXC8 transcription, thereby increasing the HOXC8 and limiting OD, proliferation, and migration of hPDLSCs with periodontitis.

1. Introduction

Periodontal diseases are common oral conditions with a worldwide prevalence of 20%–50% [1]. One of the periodontal diseases prevailing in adults is periodontitis, which is a chronic inflammatory disease and may finally lead to alveolar bone loss [2,3]. Periodontitis occurs when bacterial infection initiates immuno-inflammatory responses to clean the source of infection and repair damaged tissues [4]. The whole process activates a series of inflammatory and bone metabolism-related signaling pathways [4,5]. Destruction of the periodontium is the major cause of periodontitis and human periodontal ligament stem cells (hPDLSCs) exert significance in periodontium regeneration [6,7]. Therefore, exploring the function of hPDLSCs and the molecular mechanism of hPDLSCs injury is beneficial to the treatment of periodontal diseases.

* Corresponding author. Department of Oral Implantology and Prosthodontics, The First Affiliated Hospital of Zhengzhou University, No.1 Jianshe East Road, Erqi District, Zhengzhou, Henan Province, 450000, China.
  E-mail address: niufang08177@163.com (F. Niu).

Previous studies have demonstrated that epigenetic regulations exert effects on the differentiation of stem cells [8,9]. Epigenetic regulations include DNA methylation, histone modification, chromatin remodeling, and alteration of noncoding RNA [10]. Histone demethylases could act as epigenetic regulators for the treatment of various diseases and cancers [11,12]. Especially, KDM5A could catalyze the demethylation of methylated lysine 4 of histone H3 (H3K4me3) and plays a negative role in osteogenic differentiation (OD) during osteoporosis [13,14]. The role of histone demethylase KDM5A in the functions of hPDLSCs has not been reported at home and abroad.

microRNAs (miRNAs), a class of small non-coding RNAs, are also involved in the epigenetic regulation network [15]. Emerging evidence has verified that miRNAs also play a role in the OD of stem cells [16,17]. KDM5A is reported to bind to the miR-495 promoter and promote cell proliferation and migration in prostate cancer [18]. More importantly, previous researchers have discovered that miR-495 is upregulated in rats with periodontitis and could inhibit inflammatory reactions and enhance bone differentiation in ankylosing spondylitis [19,20]. However, the literature about the regulatory mechanism of miR495 and KDM5A in periodontal diseases is limited worldwide. In this research, we aim to figure out the role of histone demethylase KDM5A in hPDLSCs with periodontitis and find a potential therapeutic target for periodontitis.

2. Materials and methods

2.1. HPDLSCs isolation

First, 4 premolar teeth were obtained from 4 patients (19–22 years old, 2 females and 2 males) due to orthodontic treatment and placed in centrifuge tubes with precooled phosphate buffer salt (PBS) (Corning, Wuhan, Hubei, China). Teeth were washed with PBS containing 1% streptomycin (Beyotime, Shanghai, China) and 1% penicillin (Beyotime, China). The periodontal tissue was scraped from the root of the tooth with a sterile scalpel and cut into pieces with a diameter of less than 1 mm. Then, tissue pieces were washed 3 times with PBS and attached to the bottom of cell culture flasks containing α-MEM (Gibco, New York, USA) supplemented with 20% fetal bovine serum (FBS). After 4 h, the cell culture flask was flipped and tissue pieces were incubated with 5% CO_2 at 37 °C. The culture medium was changed every 3 days until the cells were grown out of the tissue. Cells were sub-cultured upon 90% confluence. All experiments used the cells of the third generation.

2.2. HPDLSCs identification

According to the instructions, Flow cytometry kits (BD Biosciences, USA) were utilized to detect cell surface markers. HPDLSCs of the third generation were incubated with fluorescence-activated cell sorting (FACS) buffer containing 2% FBS and PBS. Then, following antibodies were added to the FACS buffer: CD90 (ab23894, Abcam, Cambridge, MA, USA), CD105 (ab2529, Abcam), CD45 (ab8216, Abcam) and CD34 (ab81289, Abcam). Subsequently, flow cytometry was used to detect the signals of labeled cells and FlowJo software (Beckman Coulter, Fullerton, CA, USA) was used for data analysis.

With regard to osteogenic potential detection, hPDLSCs were seeded into 6-well plates with a density of 2×10^5/well and cultured in osteogenic induction (OI) medium [α-MEM medium containing 10% FBS, 50 μg/mL vitamin C (Sigma, CA, USA), 10 nmol/L dexamethasone (Solarbio, Beijing, China), and 10 mmol/L β-glycerophosphate]. The medium was changed every 3 days. After 28 d, the cells were fixed with 4% polyformaldehyde for 30 min and stained with 2% alizarin red (Sigma). As for adipogenic induction detection,

hPDLSCs were seeded into adipogenic induction medium [α-MEM medium containing 10% FBS, 0.2 mM indomethacin (Sigma), 2 μM dexamethasone, 0.5 mM 3-isobutyl-1-methylxanthine (Sigma) and 0.01 mg/mL insulin (Sigma)]. After 28 d, the cells were stained with oil red O (Solarbio, Beijing, China) and imaged under a microscope (Olympus IX73, Tokyo, Japan).

2.3. HPDLSCs treatment

PLKO.1-lentivirus shRNA vector targeting KDM5A and its negative control (NC) were synthesized by Open Biosystems (Thermo Fisher Scientific, Inc., Waltham, MA, USA). miR-495-3p inhibitor and NC lentiviral vector were purchased from Gene Pharma (Shanghai, China). HPDLSCs were treated with 10 μg/mL porphyromonas gingivalis lipopolysaccharide (Pg-LPS) to simulate periodontitis [21]. To explore hPDLSCs' OD ability, OI medium [α-MEM medium containing 10% FBS, 50 μg/mL vitamin C, 10 nmol/L dexamethasone, and 10 mmol/L β-glycerophosphate] was utilized and changed every 3 days. CPI-455 is a specific KDM5 inhibitor (MedChemExpress LLC, NJ, USA). IC50 is to KDM510 nM. According to the manufacturer's instructions, CPI-455 or PBS was used to treat hPDLSCs.

To analyze the role of KDM5A and miR-495-3p in the OD of hPDLSCs, hPDLSCs were treated with Pg-LPS for OI. To analyze the role of KDM5A and miR-495-3p in the proliferation and migration of hPDLSCs, Pg-LPS-treated hPDLSCs were seeded into 6-well plates and transfected with PLKO.1-lentivirus shRNA at a concentration of 60 nM.

2.4. Alkaline phosphatase (ALP) staining and ALP activity determination

HPDLSCs were fixed with polyformaldehyde for 30 min at 7 d after incubation in OI medium. Then, ALP staining kits (Beyotime) were used to stain hPDLSCs at 37 °C for 15 min. Meanwhile, at 7 d after incubation, hPDLSCs were lysed in Triton-X 100 (Solarbio, Beijing, China) and ALP activity was detected using ALP activity assay kits (Nanjing Jiancheng Bioengineering Institute, Nanjing, Jiangsu, China). Finally, the microplate reader (SPECTROstar Nano, BMG Labtech, Germany) was applied to detect the absorbance at 520 nm.

2.5. Alizarin red staining

HPDLSCs were incubated in OI medium for 14 d. Then, the cells were fixed with 70% cold ethanol for 1 h and then washed with ddH_2O_2. Next, the cells were stained with alizarin red dyeing at gentle agitation for 15 min and then washed with ddH_2O_2 5 times. To assess the degree of mineralization, hPDLSCs were rinsed in 10% (w/v) cetylpyridinium chloride (Sigma) for 1 h and quantified by spectrophotometry at a wavelength of 560 nm.

2.6. Cell counting kit-8 (CCK-8) method

CCK-8 method was applied to detect the proliferation of hPDLSCs. In brief, hPDLSCs were seeded into 96-well plates at the density of 2000 cells/well. CCK-8 solution replaced the cell culture medium at 1d, 2d, and 3d, and then a microplate reader was used to measure the absorbance at 450 nm.

2.7. Colony formation assay

To measure the colony formation ability of HPDLSCs, 250 hPDLSCs were seeded into the culture dish containing 10% FBS. After 14 d, the cells were fixed with 4% polyformaldehyde and

stained with 0.1% crystal violet (Solarbio, Beijing, China). Subsequently, the number of cell clones was counted using an inverted microscope (Leica DMi8-M, Co. Ltd., Solms, Germany).

2.8. Flow cytometry

Annexin V-fluorescein isothiocyanate (FITC) kits (BD Biosciences, San Jose, CA, USA) were used to detect cell apoptosis in strict compliance with the instructions. Briefly, hPDLSCs were detached with 0.25% trypsin and centrifuged at 800 g and the supernatant was discarded. Then, the cells were washed with 0.01 mol/L PBS and resuspended in the binding buffer. Subsequently, 1×10^6 cells were stained with 5 μL Annexin V-FITC and 10 μL propidium iodide under conditions devoid of light. Flow cytometer was used to detect cell apoptosis.

2.9. Transwell assay

The Transwell chamber was used to detect the migration ability of hPDLSCs. α-MEM medium was used to resuspend hPDLSCs at the density of 8×10^4 cells/well and then the cell suspension was placed in the upper chamber, and α-MEM with 10% PBS was added into the lower chamber. Later, the Transwell chamber was incubated with 5% CO_2 at 37 °C for 24 h. The cells that did not migrate were discarded and the remaining cells were fixed with 4% polyformaldehyde for 10 min and stained with 0.5% crystal violet. Stained cells were washed gently with tap water and counted under an inverted microscope.

2.10. Enzyme-linked immunosorbent assay (ELISA)

HPDLSCs were lysed in 0.25% trypsin and centrifuged at 16000g for 15 min to collect the supernatant. According to the manufacturer's instructions, ELISA kits were used to detect the level of tumor necrosis factor-α (TNF-α) (ab181421, Abcam), interleukin-1β (IL-1β) (ab100562, Abcam) and interleukin-10 (IL-10) (ab185986, Abcam).

2.11. Chromatin immunoprecipitation (ChIP) assay

ChIP-quantitative polymerase chain reaction (qPCR) was conducted following the standard protocol of commercial kits (Beyotime, China). Briefly, hPDLSCs were fixed with 1% formaldehyde and the cell lysis buffer was processed by ultrasound to obtain fragments. The fragments were incubated with the primary antibody KDM5A (ab194286, Abcam) or immunoglobulin G (ab133470 Abcam) at 4 °C overnight to conduct Immunoprecipitation reaction. Then, the precipitate was eluted and immunoprecipitated DNA was purified by universal DNA purification kits (TIANGEN BIOTECH Co., Ltd., Beijing, China). Purified DNA was analyzed using real time-qPCR (RT-qPCR). The enrichment level was calculated according to a previous method [22]. First, two ChIP DNA fractions were normalized to input DNA fraction, where input dilution factor was 10 as 10% of IP reaction was used as input according to the formula: ΔCt [normalized ChIP] = Ct [ChIP] − (Ct [input] Log$_2$ input dilution factor). Meanwhile, ΔCt [normalized IgG mock] was calculated for IgG (mock) sample. Lastly, the fold enrichment was calculated as 2$^{−[ΔCt \ normalized \ ChIP \ − \ ΔCt \ normalized \ mock]}$. ChIP primers: forward primer, 5′-GATGTGTTTCTCACGGTTTGCC-3′; reverse primer, 5′-CACGGTAATTGTGCATCATTTG-3′.

2.12. Dual-luciferase assay

Targetscan (http://www.targetscan.org/vert_71/) was used to predict the binding relationship between miR-495-3p and HOXC8 3'untranslated region (3′UTR). Then, GenScript (Nanjing, Jiangsu, China) was used to construct HOXC8 3′UTR-wild type (WT)/mutant type (MUT). With the aid of Lipofectamine 2000 (Invitrogen, Carlsbad, CA, USA), HOXC8 WT/MUT and miR-495-3p mimic or miR-495-3p mimic-NC (GenePharma, Shanghai, China) were transfected with 293T cells (ATCC, China). After 48 h, a Dual-luciferase reporter gene detection system was applied to assess luciferase activity.

2.13. RT-qPCR

TRIzol (Invitrogen) was used to take total RNA, and 1 μg total RNA was reversely transcribed into complementary DNA using PrimeScript™ RT kits (Takara, Japan). RT-qPCR was conducted by CFX133a (RT-qPCR assay system) (Bio-Rad Laboratories, Hercules, CA, USA) using SYBR Advantage qPCR Premix (Takara) to detect gene expression. GAPDH or U6 was set as an internal reference. The $2^{−ΔΔCt}$ method was used to calculate the relative expression [23]. Primers are shown in Table 1.

2.14. Western blot

The cells were lysed using high RIPA lysis buffer (P1003B, Beyotime, Shanghai, China) to obtain total protein. Bicinchoninic acid (BCA) kits (Beyotime) were used to detect protein concentration. Proteins were separated from sodium dodecyl sulfate-polyacrylamide gel electrophoresis and transferred to polyvinylidene fluoride membranes (Kaihong, Shenzhen, Guangdong China). The membrane blockade was conducted using Tris-buffered saline tween buffer containing 5% skim milk at 37 °C for 1 h, followed by incubation with the primary antibodies Runt-related transcription factor 2 (Runx2) (1:1000, ab236639, Abcam), osteocalcin (OCN) (1:1000, ab133612, Abcam), osteopontin (OPN) (1:1000, ab214050, Abcam), KDM5A (1:5000, ab194286, Abcam), H3K4me3 (1:1000, ab213224, Abcam) and β-actin (1:100, ab8227, Abcam). After overnight incubation with the primary antibody, the membranes were cultured with the secondary antibody (1:2000, ab6721, Abcam) at room temperature for 2 h. Finally, enhanced chemiluminescence (Thermo Fisher, Waltham, MA, USA) was used to observe Western blot, and Image J software (NIH, Bethesda, MD, USA) was used to analyze the relative expression of proteins with β-actin as the internal reference.

2.15. Statistical analysis

SPSS21.0 software (IBM Corp, Armonk, NY, USA) and GraphPad Prism 8.0 software (GraphPad Software Inc., San Diego, CA, USA) were

Table 1
Primer sequence information.

Name of primer	Sequences (5′-3′)
HOXC8	F: ATGAGCTCCTACTTCGTCAACCC
	R: TTAGTCCTTGTTTTCTTCCTTTTCC
miR-495-3p	F: AAACAAACATGGTGCACTTCTT
	R: AAGAAGTGCACCATGTTTGTTT
Runx2	F: ATGGCATCAAACAGCCTCTTCAG
	R: TCAATATGGTCGCCAAACAGAT
OCN	F : F: ATGAGAGCCCTCACACTCCTCGC
	R: CTAGACCGGGCCGTAGAAGCGC
OPN	F: ATGAGAATTGCAGTGATTTGCTT
	R: TTAATTGACCTCAGAAGATGCACTA
KDM5A	F: ATGGCGGGCGTGGGGCCGGGGGGCTA
	R: CTAACTGGTCTCTTAAGATCCTCC
GAPDH	F: ATGGTTTACATGTTCCAATATGA
	R: TTACTCCTTGGAGGCCATGTGG
U6	F: AACGATACAGAGAAGATTAGCAT
	R: TTCACGAATTTGCGTGTCATCCTT
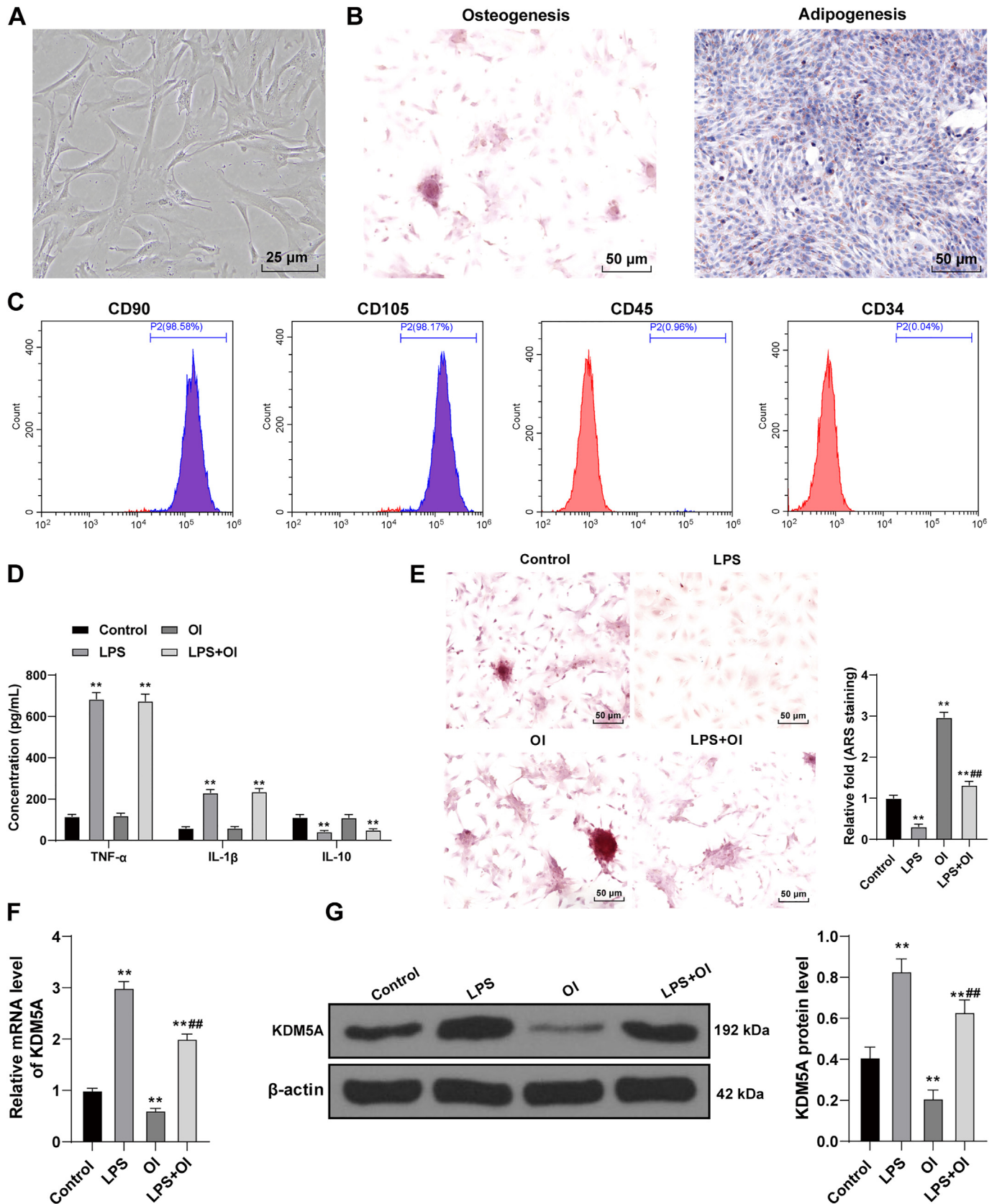
Fig. 1. KDM5A was expressed highly in hPDLSCs with periodontitis. A: The shape of hPDLSCs was observed under an inverted microscope; B: After OI and adipogenic induction, hPDLSCs were subjected to alizarin red staining and oil red O staining; C: Flow cytometry detected the expression of CD90, CD105, CD45, and CD34 in hPDLSCs; hPDLSCs were treated with Pg-LPS, followed by osteogenic induction; D: ELISA detected the level of inflammation-related cytokines; E: Alizarin red staining detected the mineralization of hPDLSCs; F–G: RT-qPCR and Western blot detected the expression patterns of KDM5A. Each cell experiment was performed 3 times and the data were represented as mean ± SD; Comparisons among multiple groups in panels E−G were analyzed using one-way ANOVA; Comparisons among multiple groups in panel D were analyzed using two-way ANOVA. All data were checked by Tukey's multiple comparisons test. **$P < 0.01$, ##$P < 0.01$, ** vs Control group, ## vs OI group. LPS: Pg-LPS; OI: osteogenic induction.
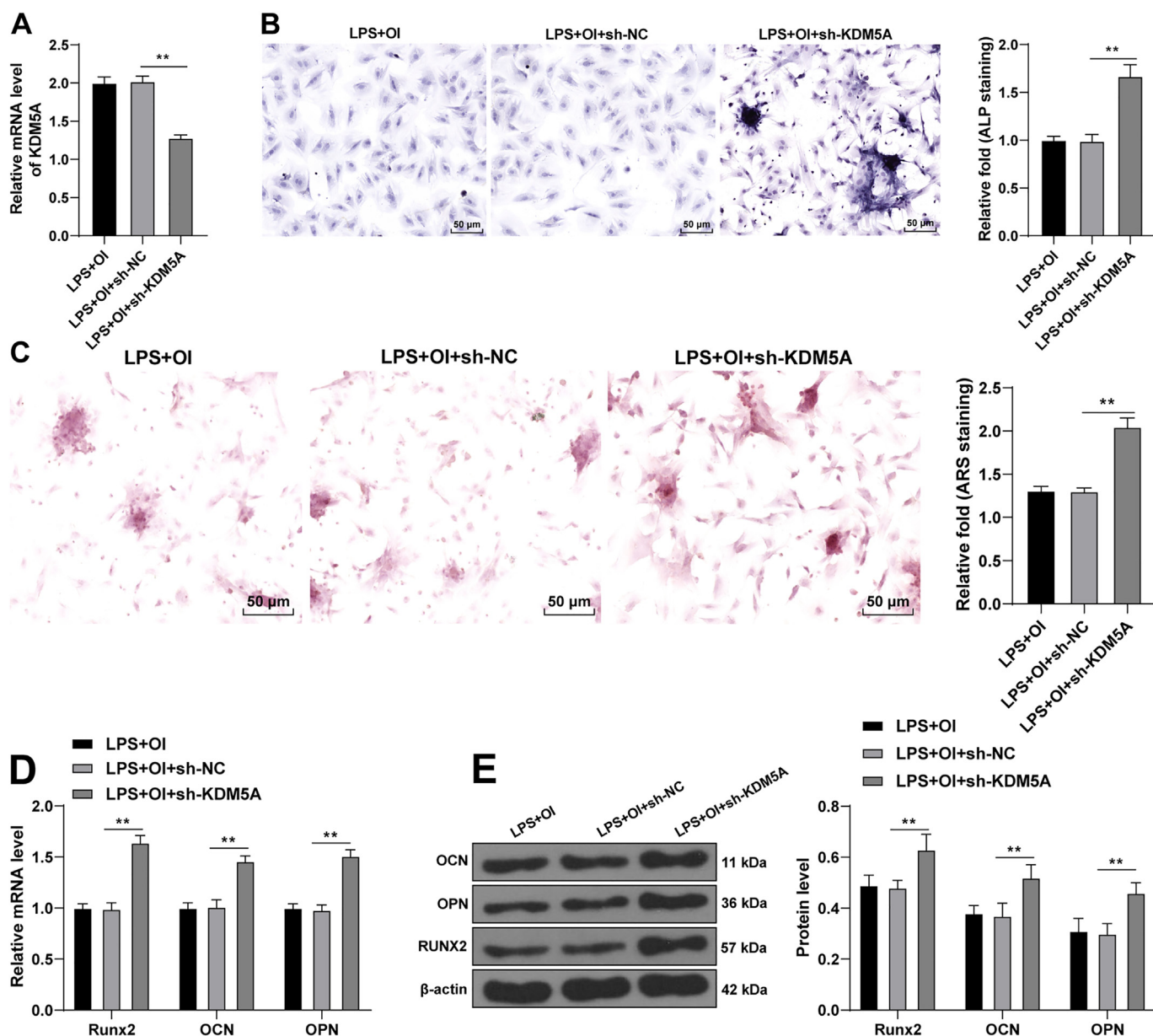
Fig. 2. Downregulation of KDM5A promoted osteogenic differentiation of hPDLSCs with periodontitis. KDM5A shRNA lentivirus was transfected into hPDLSCs in the LPS+OI group and hPDLSCs transfected with NC shRNA were set as the control. Then, samples of hPDLSCs were divided into the LPS+OI group, LPS+OI+sh-NC group, and LPS+OI+sh-KDM5A group. A: RT-qPCR detected the interference efficiency of KDM5A shRNA; B: ALP staining and ALP activity determination were conducted after 7 days of OI; C: Alizarin red staining was performed to detect mineralization of hPDLSCs after 14 days of OI; RT-qPCR (D) and Western blot (E) detected the level of Runx2, OCN and OPN in hPDLSCs. Each cell experiment was performed 3 times and data were represented as mean ± SD; Comparisons among multiple groups in panels A−C were analyzed using one-way ANOVA; Comparisons among multiple groups in panels D−E were analyzed using two-way ANOVA. All data were checked by Tukey's multiple comparisons test. **$P < 0.01$.

applied for data analysis and graphing. Data complied with normal distribution and homogeneity of variance. The data were represented as mean ± standard deviation (SD). The comparisons between multiple groups were used one-way analysis of variance (ANOVA) or two-way ANOVA and checked by Tukey's multiple comparisons test. A value of $P < 0.05$ was considered significant in statistics.

3. Results

3.1. KDM5A was expressed lowly in hPDLSCs with periodontitis

Periodontitis is a chronic inflammatory disease with high morbidity that results in tooth loss [5,24,25]. KDM5A controls OD of bone mesenchymal stem cells induced by bone morphogenetic protein 2 in osteoporosis [13]. However, the role of KDM5A in hPDLSCs under the condition of periodontitis remains unknown. Therefore, hPDLSCs were taken from the teeth of enrolled participants. Under the microscope, we observed that hPDLSCs were in the shape of fusiform or long spindle (Fig. 1A) and possessed osteogenic and adipogenic differentiation properties (Fig. 1B). According to a report [26,27], hPDLSCs were identified with markers, such as CD90. Flow cytometry showed that CD90 and CD105 were highly expressed, while CD45 and CD34 were not expressed in the cells (Fig. 1C), suggesting that hPDLSCs were successfully obtained. Then, hPDLSCs were treated with LPS to simulate periodontitis, followed by OD. ELISA showed that after the treatment of LPS, the contents of TNF-α and IL-1β were upregulated and the content of IL-10 was downregulated ($P < 0.01$, Fig. 1D). Alizarin red staining showed that mineralized
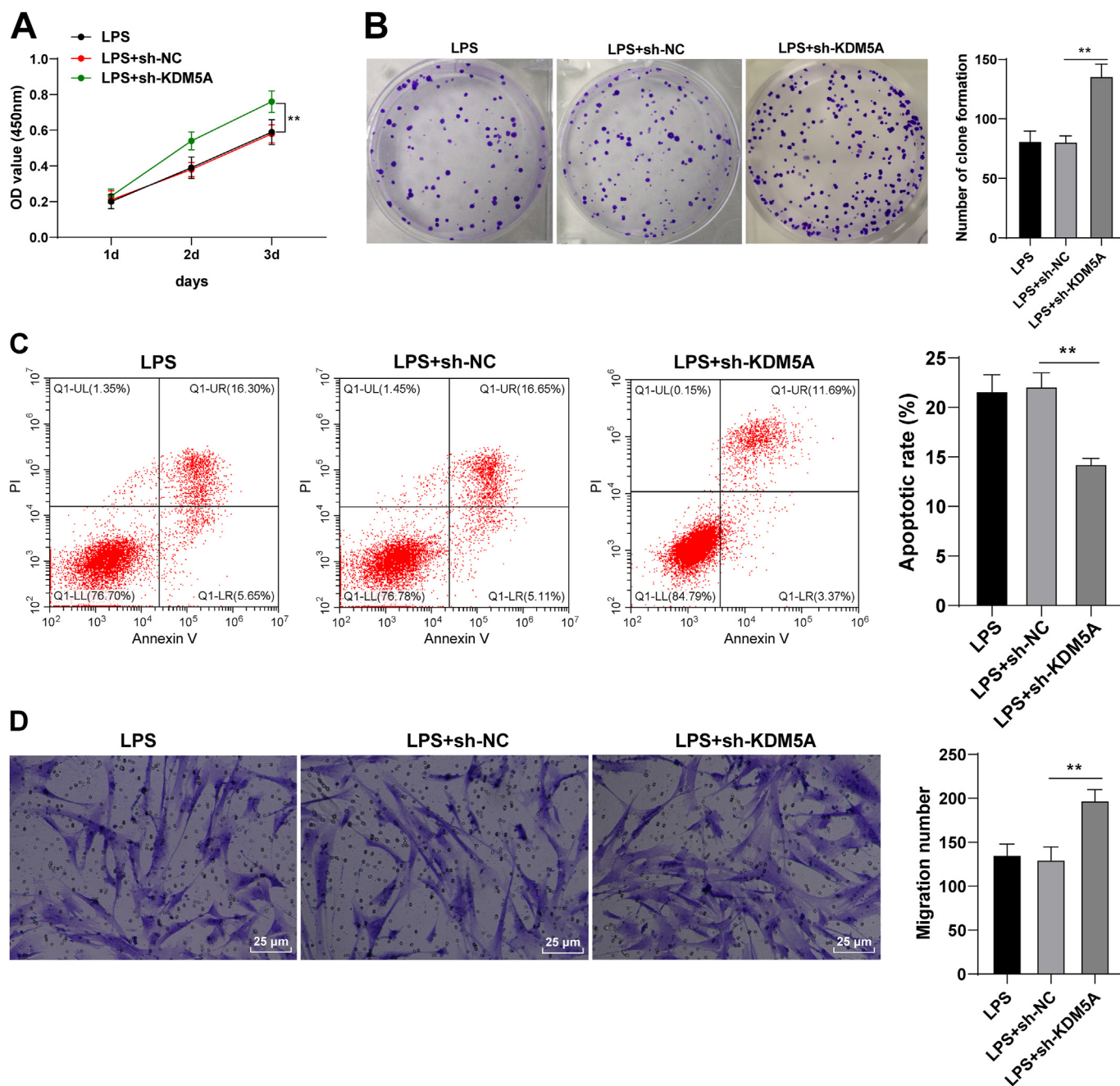
Fig. 3. KDM5A knockdown limited the apoptosis of hPDLSCs and promoted cell proliferation and migration. KDM5A shRNA lentivirus was transfected into hPDLSCs in the LPS group, and hPDLSCs transfected with NC shRNA were set as controls. Then, samples of hPDLSCs were divided into LPS group, LPS+sh-NC group, and LPS+sh-KDM5A group. A–B: CCK-8 and colony formation assay detected cell proliferation; C: Flow cytometry detected cell apoptosis; D: Transwell assay detected cell migration capacity. Each cell experiment was performed 3 times and data were represented as mean ± SD; Comparisons among multiple groups were used one-way ANOVA in panels B–D; Comparisons among multiple groups were used two-way ANOVA in panel A. All data were checked by Tukey's multiple comparisons test. **$P < 0.01$.

nodules were significantly increased after OI while reduced after LPS treatment ($P < 0.01$, Fig. 1E). Moreover, the detection of KDM5A expression showed that compared with the control group, KDM5A was highly expressed in the LPS group while weakly expressed in the OI group. Additionally, compared with the OI group, the expression of KDM5A was elevated in the LPS+OI group ($P < 0.01$, Fig. 1F–G). Taken together, KDM5A was highly expressed in hPDLSCs with periodontitis and downregulated after OI.

3.2. Downregulation of KDM5A promoted OD of hPDLSCs with periodontitis

To explore the role of KDM5A in OD of hPDLSCs with periodontitis, KDM5A shRNA were transfected with LPS-treated hPDLSCs and OI-treated hPDLSCs to downregulate the expression of KDM5A in hPDLSCs ($P < 0.01$, Fig. 2A). Then, it was observed that the activity of ALP and mineralized nodules were significantly
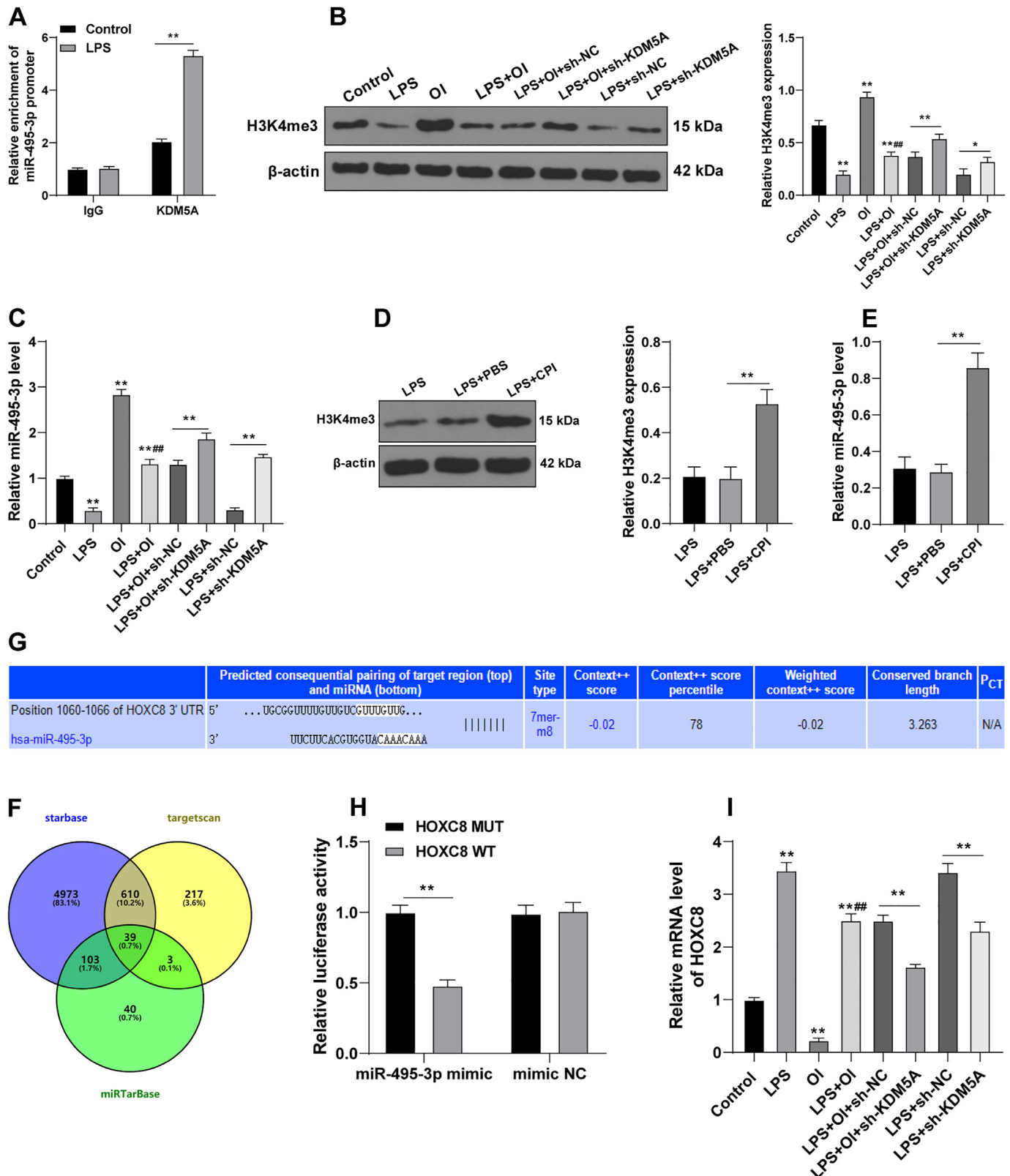
Fig. 4. KDM5A downregulated miR-495-3p expression via H3K4me3 to promote HOXC8 transcription. Samples of hPDLSCs were divided into control group, LPS group, OI group, LPS+OI group, LPS+OI+sh-NC group, and LPS+OI+sh- KDM5A group. A: ChIP assay analyzed the binding of KDM5A and miR-495-3p promoter; B: Western blot detected the expression of H3K4me3; C: RT-qPCR detected the expression of miR-495-3p in each group, and hPDLSCs in the LPS group were treated with CPI-45 with PBS treatment as the control. D: Western blot detected the level of H3K4me3; E: RT-qPCR detected the expression of miR-495-3p; F: Starbase (http://starbase.sysu.edu.cn/index.php), Targetscan (http://www.targetscan.org/vert_71/) and miRTarBase (http://mirtarbase.cuhk.edu.cn/php/search.php) predicted downstream target genes of miR-495-3p and intersections were obtained; G: Targetscan predicted the binding site of miR-495-3p and HOXC8; H: Dual-luciferase assay verified the binding relation of miR-495-3p and HOXC8; I: RT-qPCR detected the HOXC8 mRNA expression. Each cell experiment was performed 3 times and data were represented as mean ± SD; Comparisons among multiple groups were used one-way ANOVA and checked by Tukey's multiple comparisons test in panels B−E, I; Comparisons among multiple groups were used two-way ANOVA and checked by Sidak's multiple comparisons test in panels A, H. *$P < 0.05$, **$P < 0.01$, ##$P < 0.01$, ** vs Control, ## vs OI.
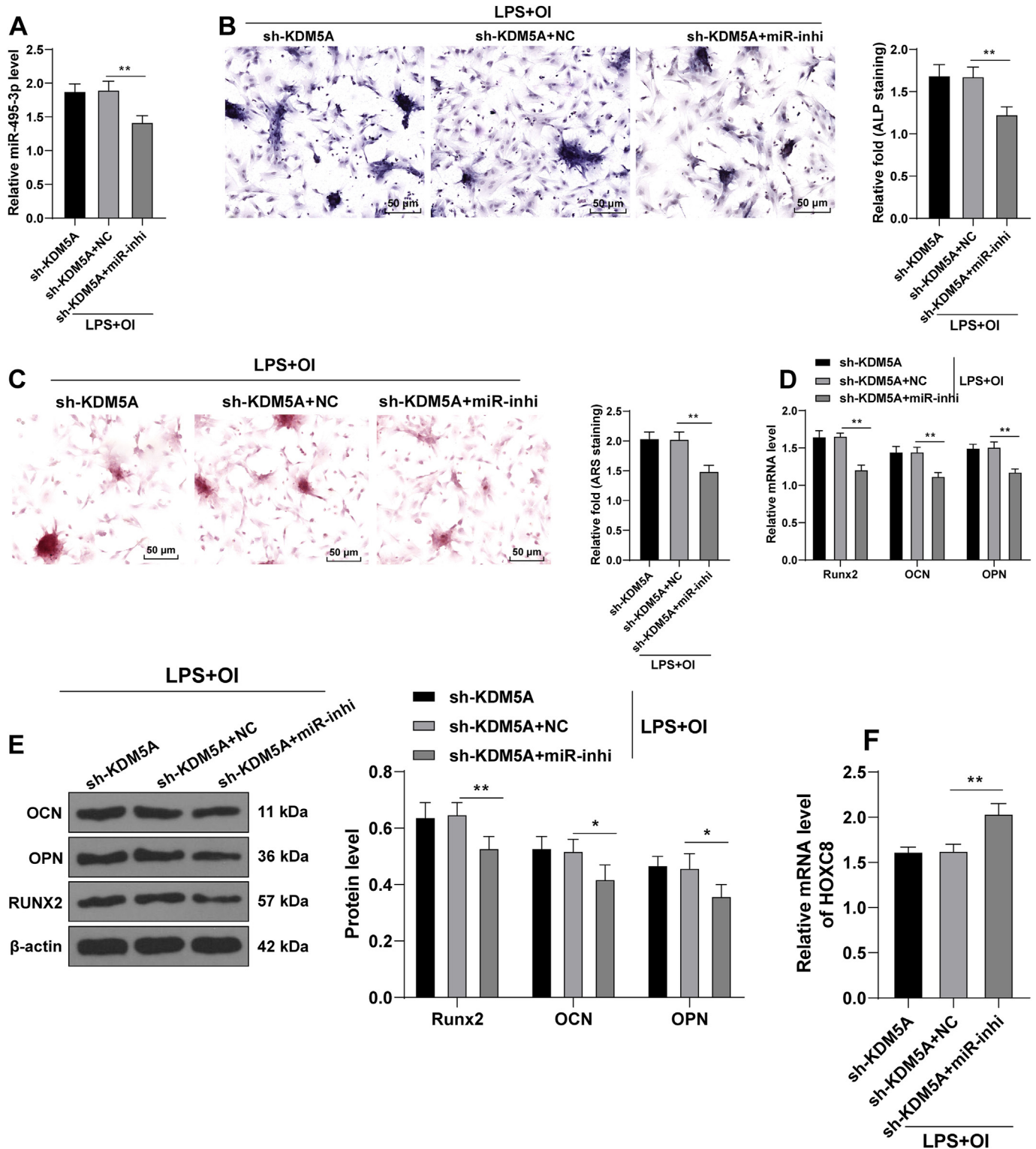
Fig. 5. miR-495-3p knockdown weakened the effect of sh-KDM5A to promote osteogenic differentiation in hPDLSCs with periodontitis. miR-495-3p inhibitor-lentivirus was transfected into hPDLSCs with NC transfection as the control. A: RT-qPCR detected the interference efficiency of miR-495-3p inhibitor; B: ALP staining and ALP activity determination were performed after 7 d of OI; C: Alizarin red staining and detection of mineralized nodules were performed after 14 d of OI; D—E: RT-qPCR and Western blot detected the expression patterns of Runx2, OCN and OPN after 14 d of OI; F: RT-qPCR detected the HOXC8 mRNA expression. Each cell experiment was performed 3 times and data were represented as mean ± SD; Comparisons among multiple groups were used one-way ANOVA in panels A—C and F; Comparisons among multiple groups were used two-way ANOVA in panel E. All data were checked by Tukey's multiple comparisons test. *$P < 0.05$, **$P < 0.01$.
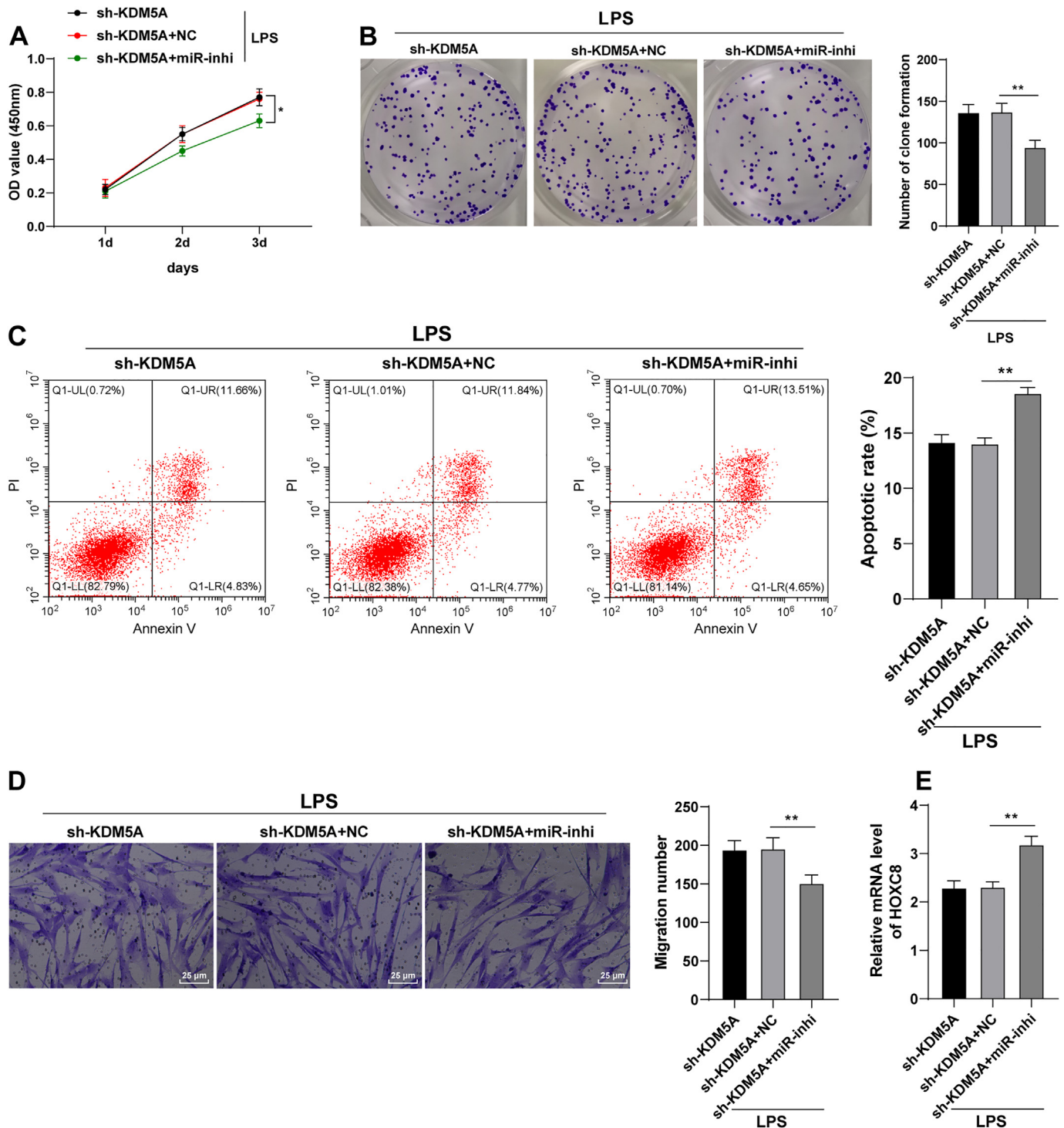
Fig. 6. miR-495-3p knockdown weakened the effect of sh-KDM5A to promote proliferation and migration of hPDLSCs with periodontitis. HPDLSCs were transfected with miR-495-3p inhibitor-lentivirus with NC transfection as the control. CCK-8 (A) method and colony formation assay (B) detected cell proliferation; C: Flow cytometry detected cell apoptosis; D: Transwell assay detected cell migration capacity; E: RT-qPCR detected the HOXC8 mRNA expression. Each cell experiment was performed 3 times and data were represented as mean ± SD: Comparisons among multiple groups were used one-way ANOVA in panel A, C-E; Comparisons between multiple groups were used two-way ANOVA in panel B. All data were checked by Tukey's multiple comparisons test. *$P < 0.05$, **$P < 0.01$.

augmented ($P < 0.01$, Fig. 2B−C). Runx2, OCN, and OPN were associated with OD [28,29]. The results showed that down-regulation of KDM5A increased the levels of Runx2, OCN and OPN ($P < 0.01$, Fig. 2D−E). In conclusion, downregulation of KDM5A could promote OD of hPDLSCs with periodontitis.

3.3. KDM5A knockdown relieved the apoptosis of hPDLSCs and promoted cell proliferation and migration

Subsequently, we explored the role of KDM5A in other aspects of hPDLSCs. Compared with the LPS+sh-NC group, proliferation

capacity of hPDLSCs in the LPS+sh-KDM5A group was significantly enhanced (P < 0.01, Fig. 3A—B). Additionally, after downregulation of KDM5A, the apoptosis index of hPDLSCs was significantly reduced (P < 0.01, Fig. 3C), while cell migration was promoted (P < 0.01, Fig. 3D). Collectively, the results suggested that KDM5A knockdown limited the apoptosis of hPDLSCs and promoted cell proliferation and migration.

3.4. KDM5A downregulated miR-495-3p expression via demethylation to promote HOXC8 transcription

According to the literature, KDM5A as the H3K4Me3 demethylase [14] could bind to the miR-495 promoter to inhibit the transcription and expression of miR-495 [18]. Therefore, we hypothesized that KDM5A influences miR-495-3p transcription via H3K4me3. The results of ChIP assay showed that KDM5A could bind to the miR-495-3p promoter (P < 0.01, Fig. 4A). Moreover, after LPS treatment, the expression patterns of H3K4me3 and miR-495-3p were significantly decreased, while OI significantly upregulated the expressions of H3K4me3 and miR-495-3p (all P < 0.01, Fig. 4B—C). Compared with the OI group, the expressions of H3K4me3 and miR-495-3p in the LPS+OI group were significantly reduced (P < 0.01, Fig. 4B—C). KDM5A knockdown increased the level of H3K4me3 and miR-495-3p (P < 0.05 Fig. 4B—C), suggesting that KDM5A regulated the expression of miR-495-3p via H3K4me3. Subsequently, CPI-455 treatment upregulated the expression of H3K4me3 in LPS-treated hPDLSCs (P < 0.01, Fig. 4D), and the expression of miR-495-3p was found to be increased simultaneously (P < 0.01, Fig. 4E). Then, Starbase, Targetscan, and miRTarBase were used to predict the downstream target genes of miR-495-3p and 39 intersections were obtained (Fig. 4F). Among these, HOXC8 regulates cell OD [30,31]. Binding site predicted by Targetscan (Fig. 4G) and dual-luciferase assay (P < 0.01, Fig. 4H) proved the binding relationship between miR-495-3p and HOXC8. Additionally, the HOXC8 mRNA expression was increased after LPS treatment while decreased after OI. Compared with the OI group, the HOXC8 mRNA expression was upregulated in the LPS+OI group. Downregulation of KDM5A resulted in reduced HOXC8 mRNA expression (P < 0.01, Fig. 4I). Altogether, KDM5A downregulated miR-495-3p expression via H3K4me3 to promote HOXC8 transcription.

3.5. miR-495-3p knockdown weakened the effect of sh-KDM5A on OD in hPDLSCs with periodontitis

To confirm the role of miR-495-3p, miR-495-3p inhibitor-lentivirus was transfected into hPDLSCs to downregulate the expression of miR-495-3p (P < 0.01, Fig. 5A). After downregulation of miR-495-3p, mineralized nodules and ALP activity were reduced (P < 0.01, Fig. 5B—C) and so did the expression of Runx2, OCN, and OPN (P < 0.05, Fig. 5D—E). Additionally, after downregulation of miR-495-3p, the HOXC8 mRNA expression was significantly increased (P < 0.01, Fig. 5F). Briefly, miR-495-3p knockdown upregulated HOXC8 and weakened the effect of sh-KDM5A to promote OD in hPDLSCs with periodontitis.

3.6. miR-495-3p knockdown weakened the effect of sh-KDM5A to promote proliferation and migration of hPDLSCs with periodontitis

Then, we focused on the role of miR-495-3p in proliferation and migration of hPDLSCs. It was observed that downregulation of miR-495-3p repressed hPDLSCs proliferation and migration (P < 0.05, Fig. 6A—D) and increased the HOXC8 mRNA expression (Fig. 6E). The results indicated that low expression of miR-495-3p upregulated the level of HOXC8 mRNA and mitigated the effect of KDM5A downregulation to promote proliferation and migration of hPDLSCs with periodontitis.

4. Discussion

Periodontitis is the sixth most common human disease that affects 11.2% of the world population [32]. The limitation of OD in hPDLSCs is a significant sign of periodontitis [33]. A previous study demonstrated that KDM5A as an epigenetic factor participates in cell differentiation [34]. In this research, we elucidated that KDM5A could promote the OD of hPDLSCs with periodontitis via regulating miR-495-3p and HOXC8.

TNF-α and IL-1β are pro-inflammatory cytokines that promote periodontitis and IL-10 is an anti-inflammatory cytokine that inhibits periodontitis [35]. In this research, hPDLSCs were treated with LPS to induce periodontitis. The results showed that the levels of TNF-α and IL-1β were increased, and the level of IL-10 and
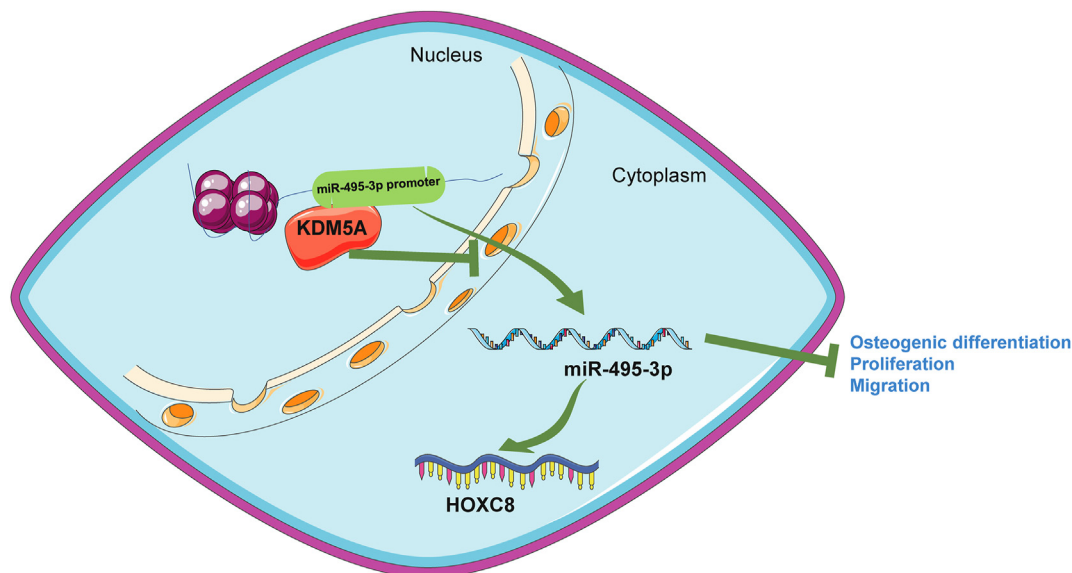
Fig. 7. Mechanism of histone demethylase KDM5A regulating hPDLSCs in periodontitis condition. KDM5A could bind to the miR-495-3p promoter and inhibit miR-495-3p level via demethylation of H3K4me3, leading to upregulation of HOXC8 mRNA and inhibition in OD, proliferation, and migration of hPDLSCs with periodontitis.

mineralized nodules were declined, indicating the infection of periodontitis. Additionally, the expression of KDM5A was upregulated in hPDLSCs with LPS treatment, but reduced after OI. Previous research has demonstrated that overexpression of KDM5A inhibits OD and bone formation of bone mesenchymal stem cells during osteoporosis [13]. Therefore, we hypothesized that KDM5A plays a negative role in the OD of hPDLSCs with periodontitis. We downregulated the expression of KDM5A in LPS-treated hPDLSCs via KDM5A shRNA and observed that ALP activity, mineralized nodules, and the expression patterns of Runx2, OCN, and OPN were all increased. Besides, after downregulation of KDM5A, the apoptosis rate of hPDLSCs was reduced and migration capacity of hPDLSCs was strengthened. Consistently, previous research reported that KDM5A knockdown improves odontogenic differentiation of human dental pulp cells with the increases in ALP and OCN [36]. Taken together, our results proved that the inhibition of KDM5A expression could promote OD of hPDLSCs with periodontitis, decline apoptosis rate and strengthen proliferation and migration.

According to the literature, miRNAs are also involved in the OD of stem cells [17]. Previous research has proved that miR-495 family promotes OD and depressed inflammatory response in ankylosing spondylitis [19]. However, the role of miR-495-3p in the OD of hPDLSCs remains known. In this research, ChIP assay confirmed that KDM5A could bind to the miR-495-3p promoter, suggesting that KDM5A could regulate miR-495-3p. The result is consistent with recent research reporting that KDM5A controls the transcription and expression of miR-495-3p [18]. Furthermore, miR-495-3p and H3K4me3 expressions were decreased after LPS treatment while increased after OI treatment, suggesting that miR-495-3p and H3K4me3 are expressed lowly in periodontitis. The results are supported by previous studies proposing that miR-495-3p and H3K4me3 have weak expressions in periodontal diseases [37,38]. Furthermore, a previous study has evidenced that KDM5A catalyzed methylation of H3K4me3 [14]. After downregulation of KDM5A, the levels of H3K4me3 and miR-495-3p were both reduced, suggesting that KDM5A regulated the miR-495-3p expression via H3K4me3. Additionally, the functional rescue experiments showed that downregulation of miR-495-3p decreased mineralized nodules, ALP activity, and expressions of Runx2, OCN, and OPN, suggesting that silencing miR-495-3p mitigated OD, proliferation, and migration of hPDLSCs induced by KDM5A knockdown. MiR-495 family was reported to participate in OD [39]. Notably, overexpression of miR-495 was demonstrated to promote proliferation and differentiation of osteoblasts in tibial fracture mice with elevations of OCN, OPN, calcium nodules, and ALP activity [40]. Altogether, silencing KDM5A upregulated miR-495-3p via methylation of H3K4me3 to promote OD, proliferation, and migration of hPDLSCs with periodontitis.

Then, we explored the downstream target gene of miR-495-3p. Through database prediction and intersection, we focused on HOXC8. A previous study has proposed that HOXC8 promoted OD in vitro via regulating bone morphogenetic protein-2 [30]. In this research, the dual-luciferase assay confirmed the targeting relationship between miR-495-3p and HOXC8. Besides, the expression of HOXC8 was decreased in hPDLSCs with LPS treatment while increased in hPDLSCs after OI treatment. Consistently, HOXC8 proteins regulated by miR-196a could facilitate proliferation and OD of human adipose-derived mesenchymal stem cells [31]. Subsequently, in the functional rescue experiment, we observed that downregulation of miR-495-3p inhibited HOXC8 transcription. In brief, KDM5A knockdown targeted miR-495-3p to upregulate HOXC8 transcription and promote OD, proliferation, and migration of hPDLSCs with periodontitis. Nevertheless, the role of HOXC8 in hPDLSC functions needs to be further discussed in future studies.

In summary, KDM5A inhibited miR-495-3p expression via demethylation of H3K4me3, thereby promoting HOXC8 transcription and limiting OD and proliferation of hPDLSCs with periodontitis (Fig. 7). Although the research revealed the role of KDM5A and miR-495-3p in the functions of hPDLSCs, we did not investigate whether other demethylases, miRNAs, and downstream target genes exert effects in hPDLSCs. Besides, since our study is the first attempt to explore the role of KDM5A in the functions of hPDLSCs with periodontitis, we just preliminarily explore the downstream mechanism of KDM5A at the cell level. In the future, we will fully investigate the upstream and downstream mechanisms of KDM5A to improve the integrity of our study about the role of KDM5A in periodontitis.

Ethical approval

All experimental procedures in this study were approved by the Ethics Committee of The First Affiliated Hospital of Zhengzhou University. All participants were informed of the experiment and signed the consent.

Funding

Availability of data and materials

The data that support this study are available from the corresponding author upon reasonable request.

Declaration of competing interest

The authors declare no conflict of interest.

Acknowledgments

References

[1] Nazir MA. Prevalence of periodontal disease, its association with systemic diseases and prevention. Int J Health Sci (Qassim) 2017;11:72—80.
[2] Wang CJ, McCauley LK. Osteoporosis and periodontitis. Curr Osteoporos Rep 2016;14:284—91.
[3] Cardoso EM, Reis C, Manzanares-Cespedes MC. Chronic periodontitis, inflammatory cytokines, and interrelationship with other chronic diseases. Postgrad Med 2018;130:98—104.
[4] Mo LY, Jia XY, Liu CC, Zhou XD, Xu X. Role of autophagy in the pathogenesis of periodontitis. Hua Xi Kou Qiang Yi Xue Za Zhi 2019;37:422—7.
[5] Zhang J, Zhang AM, Zhang ZM, Jia JL, Sui XX, Yu LR, et al. Efficacy of combined orthodontic-periodontic treatment for patients with periodontitis and its effect on inflammatory cytokines: a comparative study. Am J Orthod Dentofacial Orthop 2017;152:494—500.
[6] Liu J, Yu F, Sun Y, Jiang B, Zhang W, Yang J, et al. Concise reviews: characteristics and potential applications of human dental tissue-derived mesenchymal stem cells. Stem Cell 2015;33:627—38.
[7] Tomokiyo A, Wada N, Maeda H. Periodontal ligament stem cells: regenerative potency in periodontium. Stem Cell Dev 2019;28:974—85.
[8] Verzi MP, Shivdasani RA. Epigenetic regulation of intestinal stem cell differentiation. Am J Physiol Gastrointest Liver Physiol 2020;319:G189—96.
[9] Atlasi Y, Stunnenberg HG. The interplay of epigenetic marks during stem cell differentiation and development. Nat Rev Genet 2017;18:643—58.
[10] Alvarez-Errico D, Vento-Tormo R, Sieweke M, Ballestar E. Epigenetic control of myeloid cell differentiation, identity and function. Nat Rev Immunol 2015;15:7—17.
[11] Lee DH, Kim GW, Jeon YH, Yoo J, Lee SW, Kwon SH. Advances in histone demethylase KDM4 as cancer therapeutic targets. FASEB J 2020;34:3461—84.
[12] Chen H, Huang Y, Zhu X, Liu C, Yuan Y, Su H, et al. Histone demethylase UTX is a therapeutic target for diabetic kidney disease. J Physiol 2019;597:1643—60.

[13] Wang C, Wang J, Li J, Hu G, Shan S, Li Q, et al. KDM5A controls bone morphogenic protein 2-induced osteogenic differentiation of bone mesenchymal stem cells during osteoporosis. Cell Death Dis 2016;7:e2335.

[14] Petronikolou N, Longbotham JE, Fujimori DG. Extended recognition of the histone H3 tail by histone demethylase KDM5A. Biochemistry 2020;59: 647—51.

[15] Morales S, Monzo M, Navarro A. Epigenetic regulation mechanisms of microRNA expression. Biomol Concepts 2017;8:203—12.

[16] Lin Z, He H, Wang M, Liang J. MicroRNA-130a controls bone marrow mesenchymal stem cell differentiation towards the osteoblastic and adipogenic fate. Cell Prolif 2019;52:e12688.

[17] Zhang Z, Wang N, Zhang Y, Zhao J, Lv J. Downregulation of microRNA-302b-3p relieves oxygen-glucose deprivation/re-oxygenation induced injury in murine hippocampal neurons through up-regulating Nrf2 signaling by targeting fibroblast growth factor 15/19. Chem Biol Interact 2019;309:108705.

[18] Du C, Lv C, Feng Y, Yu S. Activation of the KDM5A/miRNA-495/YTHDF2/m6A-MOB3B axis facilitates prostate cancer progression. J Exp Clin Cancer Res 2020;39:223.

[19] Du W, Yin L, Tong P, Chen J, Zhong Y, Huang J, et al. MiR-495 targeting dvl-2 represses the inflammatory response of ankylosing spondylitis. Am J Transl Res 2019;11:2742—53.

[20] Tomofuji T, Yoneda T, Machida T, Ekuni D, Azuma T, Kataoka K, et al. MicroRNAs as serum biomarkers for periodontitis. J Clin Periodontol 2016;43: 418—25.

[21] Liu Z, He Y, Xu C, Li J, Zeng S, Yang X, et al. The role of PHF8 and TLR4 in osteogenic differentiation of periodontal ligament cells in inflammatory environment. J Periodontol 2021;92:1049—59.

[22] Kumar A, Dumasia K, Deshpande S, Balasinor NH. Direct regulation of genes involved in sperm release by estrogen and androgen through their receptors and coregulators. J Steroid Biochem Mol Biol 2017;171:66—74.

[23] Livak KJ, Schmittgen TD. Analysis of relative gene expression data using real-time quantitative PCR and the 2(-Delta Delta C(T)) Method. Methods 2001;25: 402—8.

[24] Ahmad N, Ahmad FJ, Bedi S, Sharma S, Umar S, Ansari MA. A novel Nano-formulation Development of Eugenol and their treatment in inflammation and periodontitis. Saudi Pharm J 2019;27:778—90.

[25] Serrano C, Suarez E. Prevalence of severe periodontitis in a Colombian adult population. J Int Acad Periodontol 2019;21:53—62.

[26] Zhao B, Zhang W, Xiong Y, Zhang Y, Zhang D, Xu X. Effects of rutin on the oxidative stress, proliferation and osteogenic differentiation of periodontal ligament stem cells in LPS-induced inflammatory environment and the underlying mechanism. J Mol Histol 2020;51:161—71.

[27] Jia L, Zhang Y, Ji Y, Xiong Y, Zhang W, Wen Y, et al. YAP balances the osteogenic and adipogenic differentiation of hPDLSCs in vitro partly through the Wnt/beta-catenin signaling pathway. Biochem Biophys Res Commun 2019;518:154—60.

[28] Wu Y, Zhu T, Yang Y, Gao H, Shu C, Chen Q, et al. Irradiation with red light-emitting diode enhances proliferation and osteogenic differentiation of periodontal ligament stem cells. Laser Med Sci 2021;36:1535—43.

[29] Liu S, Yang X, Zhong X, Li L, Zhang X. Involvement of miR-337 in high glucose-suppressed osteogenic differentiation in bone marrow mesenchymal stem cells via negative regulation of Rap1A. In Vitro Cell Dev Biol Anim 2021;57:350—8.

[30] Zheng YJ, Chung HJ, Min H, Kang M, Kim SH, Gadi J, et al. In vitro osteoblast differentiation is negatively regulated by Hoxc8. Appl Biochem Biotechnol 2010;160:891—900.

[31] Kim YJ, Bae SW, Yu SS, Bae YC, Jung JS. miR-196a regulates proliferation and osteogenic differentiation in mesenchymal stem cells derived from human adipose tissue. J Bone Miner Res 2009;24:816—25.

[32] Sanz M, Del Castillo AM, Jepsen S, Gonzalez-Juanatey JR, D'Aiuto F, Bouchard P, et al. Periodontitis and cardiovascular diseases. Consensus report. Glob Heart 2020;15:1.

[33] Sun J, Liu Y, Qu Q, Qu J, Luo W, Zhang F, et al. Effect of histone acetylation on osteogenic differentiation of periodontal ligament stem cells derived from periodontitis tissue. Hua Xi Kou Qiang Yi Xue Za Zhi 2019;37:102—5.

[34] Guo L, Guo YY, Li BY, Peng WQ, Tang QQ. Histone demethylase KDM5A is transactivated by the transcription factor C/EBPbeta and promotes pre-adipocyte differentiation by inhibiting Wnt/beta-catenin signaling. J Biol Chem 2019;294:9642—54.

[35] Ramadan DE, Hariyani N, Indrawati R, Ridwan RD, Diyatri I. Cytokines and chemokines in periodontitis. Eur J Dent 2020;14:483—95.

[36] Zhou C, Zhang Z, Zhu X, Qian G, Zhou Y, Sun Y, et al. N6-Methyladenosine modification of the TRIM7 positively regulates tumorigenesis and chemo-resistance in osteosarcoma through ubiquitination of BRMS1. EBioMedicine 2020;59:102955.

[37] Francis M, Pandya M, Gopinathan G, Lyu H, Ma W, Foyle D, et al. Histone methylation mechanisms modulate the inflammatory response of periodontal ligament progenitors. Stem Cell Dev 2019;28:1015—25.

[38] Du A, Zhao S, Wan L, Liu T, Peng Z, Zhou Z, et al. MicroRNA expression profile of human periodontal ligament cells under the influence of Porphyromonas gingivalis LPS. J Cell Mol Med 2016;20:1329—38.

[39] Xu X, Jiang H, Li X, Wu P, Liu J, Wang T, et al. Bioinformatics analysis on the differentiation of bone mesenchymal stem cells into osteoblasts and adipo-cytes. Mol Med Rep 2017;15:1571—6.

[40] Zhu L, Lin ZW, Wang G, Zhang H, Liu B, Xu QJ. MicroRNA-495 downregulates AQP1 and facilitates proliferation and differentiation of osteoblasts in mice with tibial fracture through activation of p38 MAPK signaling pathway. Sci Rep 2019;9:16171.